



A significant antibiofilm and antimicrobial activity of chitosan-polyacrylic acid nanoparticles against pathogenic bacteria

O'la AL-Fawares^{a,*}, Areen Alshweiat^b, Rozan O. Al-Khresieh^a, Kawthar Z. Alzarieni^c,
Ayat Hussein B. Rashaid^d

^a Department of Medical Laboratory Analysis, Faculty of Science, Al-Balqa Applied University, 19117 Al-salt, Jordan

^b Department of Pharmaceutics and Pharmaceutical Technology, Faculty of Pharmaceutical Sciences, The Hashemite University, 13133 Zarqa, Jordan

^c Department of Medicinal Chemistry and Pharmacognosy, Faculty of Pharmacy, Jordan University of Science and Technology, 22110 Irbid, Jordan

^d Department of Chemistry, Faculty of Science and Arts, Jordan University of Science and Technology, 22110 Irbid, Jordan

ARTICLE INFO

Keywords:

Campylobacter jejuni
Biofilm inhibition
Chitosan
Antibiotic resistance
Nanoparticles

ABSTRACT

Chitosan is known to exert antimicrobial activity without the need for any chemical modification; however, new derivatives of chitosan can be created to target multi-drug resistant bacteria. In this study, chitosan (CS) was cross-linked with sodium tripolyphosphate to form nanoparticles, which were then coated with polyacrylic acid (PAA). The SEM images revealed that the CS-PAA nanoparticles had spherical shapes with smooth surfaces and the size of the dried nanoparticles was approximately 222 nm. Biofilm formation was significantly inhibited by 0.5 mg/mL of CS-PAA. *In-situ* optical microscopy showed that CS-PAA nanoparticles inhibited the bacterial biofilm formation in *Campylobacter jejuni*, *Pseudomonas aeruginosa*, and *Escherichia coli* after a single treatment with 40 µg. Additionally, 20 µg of CS-PAA nanoparticles demonstrated antibacterial activity against the growth of *C. jejuni*, *P. aeruginosa*, and *E. coli* with notable inhibitory zones of 9, 12, and 13 mm, respectively ($P < 0.01$). The development of a novel and ecofriendly method for the preparation of chitosan nanoparticles through an interaction of chitosan with PAA shows promise tool to combat bacterial infections and validates effective antibacterial and antibiofilm properties against antibiotic resistant pathogens.

1. Background

Biofilms are polymeric structures created by bacteria using proteins, extracellular polysaccharides, and extracellular DNA (e-DNA) (Elga-moudi and Korolik, 2021; MubarakAli et al., 2015; Zhong et al., 2020). In nature, diverse bacteria collaborate to construct these biofilms. For instance, *C. jejuni* is recognized as an important contributor to gastro-enteritis and, in certain instances, may trigger the development of autoimmune conditions such as Guillain-Barré syndrome (GBS) and Miller Fisher syndrome during the transmission process (Al-khresieh et al., 2023; Kemper and Hensel, 2023; Zhong et al., 2020). These biofilms shield the bacteria from various environmental stresses like UV radiation, desiccation, dehydration, as well as antibacterial and sanitizing agents, therefore, confirming their survival (Oh et al., 2019). Growing as a biofilm allows bacteria to demonstrate up to 1000-fold reduction in susceptibility to antibiotics (Hughes and Webber, 2017). Numerous internal and external factors, such as the surface properties of

the substance on which the bacteria are growing, temperature, and oxygen levels, can contribute to the creation of *C. jejuni* biofilm and make their removal challenging (Stetsenko et al., 2019). Once a biofilm has established itself on a surface, it becomes more difficult to remove, requiring more aggressive eradication methods (Kim et al., 2019). As a result of the extensive and inappropriate use of antibiotics the bacterial-resistant strains has become a key concern (Mancuso et al., 2021; Paulsamy et al., 2023). The effectiveness of antibiotics in killing bacteria has become increasingly limited (Ahmed et al., 2023). In order to eliminate intracellular bacteria, higher concentrations of antibiotics are often required, potentially leading to side effects and toxicity (Kamat and Kumari, 2023; MubarakAli et al., 2015; Radwan et al., 2023).

Subsequent studies were conducted to examine biologically-derived antibiofilm and antimicrobial molecules that are biocompatible, biodegradable, non-toxic, non-allergenic, cost effective, and environmentally friendly. Recently, chitosan (CS), which is considered as an attractive biopolymer of multiple reactive groups that enables the development of

Peer review under responsibility of King Saud University

* Corresponding author.

E-mail address: ola.alfawares@bau.edu.jo (O. AL-Fawares).

<https://doi.org/10.1016/j.jsps.2023.101918>

Received 2 October 2023; Accepted 12 December 2023

Available online 13 December 2023

1319-0164/© 2023 The Authors. Published by Elsevier B.V. on behalf of King Saud University. This is an open access article under the CC BY-NC-ND license (<http://creativecommons.org/licenses/by-nc-nd/4.0/>).

drug carriers with different physicochemical aspects such as charge, hydrophobicity, and particle size (Sultan et al., 2023). Indeed, CS has successfully been introduced as a nanocarrier for several drugs and vaccines for various routes of administration, including oral, nasal, and ocular (Alalawi et al., 2019). The CS-based nanoparticles showed controlled release and longer resident time particularly for the intranasal and oral delivery, facilitating drug absorption (Cheung et al., 2015). Moreover, these nanosystems showed valuable antimicrobial and anti-biofilm activities against several microorganisms, including *Listeria monocytogenes*, *Bacillus cereus*, and *Enterococcus faecalis* (Dolnicar et al., 2015). CS nanoparticles loaded with antibiotics like gentamicin exhibited a synergistic antibiofilm activity against *L. monocytogenes* biofilms (Mu et al., 2014a). Additionally, oxacillin and chrysin CS-based formulations were effective against *Staphylococcus aureus* (Dolnicar et al., 1997; Siddhardha et al., 2020), while mikacin, vancomycin, and erythromycin formulations had efficacy against *L. monocytogenes* (Mu et al., 2014b). The activity of CS-based nanoparticles is not restricted to delivery of antibiotics, but it also extended to the adsorption of inorganic and organic compounds from aqueous solutions and to the eradication of several microorganisms from water, including *P. aeruginosa*, *E. coli*, *C. albicans*, and *S. aureus*. The nanocomposite of grafted CS showed effective adsorption of lead ions (Pb^{+2}) and methylene blue from water. These findings highlighted the various applications of CS nanosystems (Abd El-Aziz et al., 2023, 2022).

Despite the versatile use of chitosan nanoparticles, their importance in drug delivery, and their antimicrobial and antibiofilm activity, challenges related to stability are raised for these nanosystems, mainly because of their charge. CS is a cationic polymer that imparts a positive charge to the nanoparticles (Esim et al., 2018). Therefore, these nanoparticles could interact significantly with serum components. Consequently, aggregation and rapid clearance could be encountered, contributing to the low activity of these nanoparticles (Wu et al., 2017a). Surface modification of CS nanoparticles with PAA could improve the stability of the small CS nanoparticles via a simple and versatile method, constructed under mild conditions without heat or organic solvents. Moreover, this modification could preserve the integrity of the CS core, producing an efficient carrier with high loading efficiency for drugs such as antibiotics. It is worth noting that these systems exhibit a pH-dependent solubility, which could be beneficial in drug targeting (Freidin et al., 2005; Ijaz et al., 2022).

Various CS-coated microspheres have been reported as systems of antibiofilm and/or antimicrobial activity against multi-drug resistant microbial pathogens, including CS-alginate (Thaya et al., 2018) and Cinnamaldehyde-coated chitosan (Xu et al., 2022). PAA is a non-toxic, biodegradable, biocompatible, and cheap polymer (Karolewicz, 2016). It is commonly utilized in the biomedical field and in drug delivery (Xiao et al., 2012). PAA is considered chemically inert due to the absence of reactive functional groups. Interpolymer complexes and polyelectrolyte complexes (PEC), are spontaneously developed by mixing polycations and polyanions in solutions. The electrostatic interactions between oppositely charged microdomains of polyionic components drive the intermolecular forces for complexation. Other interactions, including hydrogen bonding, hydrophobic interactions, van der Waals forces and dipole interactions, contribute to the complex formation. Because of the interaction between polymers with opposing charges, the PEC coatings improve the surface characteristics of the biomaterial. PEC can modulate the antibacterial activity of polymers (Durmaz et al., n.d.; TopuzoGullari, 2020). Ortega Ortiz et al reported the enhanced antibacterial activity of CS-PAA PEC against *P. aeruginosa* and *P. oleovorans* compared to CS nanoparticles (Ortega-Ortiz et al., 2010). In a study conducted by Belbekhouche et al., a CS-PAA complex was produced as a promising delivery system for antibiotics (Belbekhouche et al., 2018). The enhancement of antimicrobial and antibiofilm activity by grafted PAA may be attributed to their composition, with a particular emphasis on the presence of free carboxylic acid functionalities. The carboxylic acid could interact with the cell wall of bacteria, thereby contributing to their

antimicrobial activity (Ortega-Ortiz et al., 2010).

Due to the emergence of multidrug-resistant microbes and lack of new antimicrobial drugs in the market, there is an urgent need to discover and develop novel and more potent antimicrobial compounds. This study aimed to investigate the antibiofilm and antimicrobial effects of CS-PAA nanoparticles on *C. jejuni* and other pathogenic gram-negative bacteria. Therefore, chitosan was first cross-linked with TPP and then complexed with PAA. The characteristics of CS-PAA nanoparticles and their antibiofilm and antimicrobial activities against multiple pathogenic strains were measured. This study reports on the synthesis of novel biosynthesized CS-PAA nanoparticles, elucidating their morphological and structural characteristics, along with their application in the medical field.

2. Materials and methods

2.1. Materials

Chitosan with deacetylation degree of 95% was purchased from Santa Cruz Biotechnology (USA), polyacrylic acid (PAA) of MW 72.06 g/mol was obtained from Sigma-Aldrich (USA), Trehalose was obtained from Combi Blocks (USA), sodium triphosphate (TPP) was obtained from Thermo Fisher Scientific (China), carbodiimide was purchased from Thermo Fisher Scientific (China). Acetic acid (CH_3COOH) and sodium hydroxide (NaOH) were purchased from Thermo Fisher Scientific (Waltham, MA, USA). Ethanol, acetone and all the reagents used were analytical grade. *C. jejuni* ATCC 33560 was obtained from the Jordan Food and Drug Administration, *P. aeruginosa* ATCC 12453 and *E. coli* ATCC 25922 were attained from the microbiology laboratory at the Jordan University of Science and Technology.

2.2. Preparation of strains

P. aeruginosa ATCC 12453 and *E. coli* ATCC 25922 were used to co-culture with *C. jejuni* ATCC 33560. *C. jejuni* was cultured on Melluler-Hinton agar (Oxoid, Thermo Fisher, Hampshire, UK) under micro-aerophilic conditions (5% N_2 , 10% CO_2 , and 85% O_2) using CampyGen bags (Oxoid, Hampshire, UK) at 42 °C for 48 h. *E. coli* and *P. aeruginosa* were also cultured on the same medium under aerobic conditions and incubated at 37 °C for 24 h (Karruli et al., 2023; Suwono et al., 2021). A single colony from each bacterial culture was sub-cultured in Melluler-Hinton broth (Oxoid, Thermo Fisher, Hampshire, UK) and kept under the desired conditions for growth, then an equal volume was extracted from each broth to attain an absorbance of 0.063 at 600 nm, which was then used for co-culture purposes.

2.3. Preparation of CS-PAA nanoparticles

The preparation of PAA-coated CS nanoparticles was carried out in two steps. Firstly, CS-TPP nanoparticles were prepared by an ionic gelation method which based on the electrostatic interaction between the positively charged chitosan and the negatively charged TPP (Wu et al., 2017). 0.01 mg/ml of CS in aqueous acetic acid solution (1, w/v %) was prepared and left on magnetic stirrer for 24 h. Then, the pH of this solution was adjusted to 6.0 by using sodium hydroxide. The CS in the prepared solution was cross-linked with 1% TPP. Then, the mixture was centrifuged at 15,000 rpm at 4 °C for 1.5 h and suspended with PAA using an Ultrasonic processor for 5 min. In the second step, the PAA and CS-TPP were combined through electrostatic attraction. Ten mg/mL carbodiimide solution was added to the earlier prepared CS-PAA nanoparticles to cross-link the CS-TPP particles with the PAA and kept overnight on stirring mode to ensure the adhesion of PAA coating onto CS-TPP through the formation of an amide bond between the carboxyl group of PAA and the amino group of the chitosan surface. Finally, the pH was adjusted within the range of 4.2 to 6.5 and the solution was ultracentrifuged for another 1.5 h at 4 °C, the supernatant was then

discarded and the CS-PAA nanoparticles were resuspended in sterile water using an ultrasonic processor.

2.4. Freeze drying of CS-PAA nanoparticles

Freeze-drying was applied to get dry CS-PAA nanoparticles using Telstar, Lyo Alfa 15–85 plus type apparatus (Telstar, Barcelona, Spain). 3% (w/v) of trehalose was added to the nano-suspensions before deep freezing. The nano-suspensions were frozen in a round-bottom flask using a deep freezer at a temperature of $-80\text{ }^{\circ}\text{C}$ for 24 h. The samples were then freeze-dried for 24 h at 0.1 mbar to produce the dry powder.

2.5. Characterization of the CS-PAA nanoparticles

2.5.1. Mean particle size (MPS) and zeta potential (ZP) analysis

The MPS and ZP of the particles were measured by laser diffraction by using a Nicomp® Nano ZLS System (Entegris, USA) using water as the dispersant and setting the refractive index to 1.33. The nanosuspensions were diluted by distilled water and measured at $25\text{ }^{\circ}\text{C}$. Twelve parallel measurements were carried out.

2.5.2. Scanning Electron microscopy (SEM)

Scanning Electron Microscopy (SEM) images were analyzed to determine the size of the dry nanoparticles. One hundred particles were selected from the SEM image and the MPS was measured by using Image J software (NIH, USA). Quanta 450 SEM (FEI, Hillsboro, OR, USA) captured images of the prepared CS-PAA nanoparticles in high-vacuum mode. The samples were mounted on aluminum stubs by double-sided adhesive sticky disks of conductive carbon, and then the particles were sputter coated with palladium to generate a 5 nm thick coating (Quorum Q 150 R, Sussex, UK). The images were captured at 10.00 kV.

2.5.3. Attenuated total reflectance-Fourier-transform infrared spectroscopy (ART-FTIR)

To evaluate the interaction between chitosan and PAA, CS-PAA nanoparticles were freeze-dried without the addition of trehalose under the same freeze-drying conditions described in Section 2.4. Powdered samples of CS, PAA, and CS-PAA nanoparticles were analyzed by ART-FTIR (Bruker Alpha, USA) spectrometer.

2.6. Biofilm measurement by crystal violet staining

The three bacterial strains (*C. jejuni* ATCC 33560, *P. aeruginosa* ATCC 12453, and *E. coli* ATCC 25922) existing in each sample were cultivated both separately and combined. Mixed culture of *C. jejuni* and either *P. aeruginosa* or *E. coli* was treated with three concentrations (0.005, 0.05, and 0.5 mg/mL) of CS-PAA nanoparticles in 96-well plates. There were 180 μL of MH broth and 20 μL of bacterial culture in each well. The bacteria were cultivated aerobically for 72 h at $37\text{ }^{\circ}\text{C}$. The 96-well plates were gently washed three times with distilled water to remove the medium. Then they were dried at $55\text{ }^{\circ}\text{C}$ for around 30 min. Staining was conducted by adding 200 μL of 0.1% crystal violet dye (Merck KGaA, Germany) to each well and incubating at room temperature for 10–15 min. Excess crystal violet was rinsed out of the wells using sterile water, and they were then dried at a temperature of $55\text{ }^{\circ}\text{C}$. A microplate reader (Bio-Tek, USA) was used to measure the optical density at 630 nm after 300 μL of an eluent (80% ethanol and 20% acetone) was applied (Zhong et al., 2020).

2.7. In-situ microscopic study

Selected bacteria were grown in biofilms on sterilized microscope slides that were submerged in nutrient broth and cultured at $37\text{ }^{\circ}\text{C}$ for 42 h for optical microscopic analysis. Following incubation, 40 g of CS-PAA nanoparticles were added to each slide. The control slide was maintained without CS-PAA nanoparticles and subjected to another

incubation at $37\text{ }^{\circ}\text{C}$ for 24 h before being observed under light microscopy. The biofilm of the samples (control and treated) was washed with phosphate-buffered saline (PBS) to get rid of any loosely-adhered cells before being stained with 1.5 mL of 0.4% crystal violet staining solution. Nikon's ECLIPSE TS 100 light microscope was used to see glass slides that had been stained with crystal violet at a 100x oil lens magnification (Anjugam et al., 2016).

2.8. Determination of antimicrobial assay

By using a well diffusion assay, the biosynthesized CS-PAA nanoparticles were tested for their antibacterial efficacy against the bacteria *C. jejuni* ATCC 33560, *P. aeruginosa* ATCC 12453, and *E. coli* ATCC 25922. Overnight-grown bacterial cultures were inoculated in solid Miller-Hinton Agar and then swabbed evenly using a sterile L-shaped rod to obtain uniform bacterial growth. On an agar plate, 6 mm holes were made, and 120 μL of 20 $\mu\text{g}/\text{ml}$ of CS-PAA nanoparticles were added. The diameter of the zone of inhibition in millimeters (mm) was used to evaluate the growth-inhibitory effect of CS-PAA nanoparticles.

2.9. Statistical analysis

The SPSS program, version 19.0 (Chicago, IL, USA), was used for data analysis. T-tests were conducted to assess the effect of varying concentrations of CS-PAA nanoparticle treating on bacterial biofilms. The threshold for statistical significance was set at a p value < 0.05 .

3. Results

3.1. Size and ZP measurements of the CS-PAA nanoparticles

The prepared suspension of the particles showed an MPS of $2.98 \pm 0.57\text{ }\mu\text{m}$ using the particle size analyzer. However, data obtained from the SEM images showed that particles had a mean particle size of $222.119 \pm 70\text{ nm}$. The particles showed ZP values of $+42.35 \pm 7.85\text{ mV}$.

3.2. Scanning Electron microscopy (SEM)

The SEM image of CS-PAA nanoparticles (Fig. 1) reveals the presence of nearly spherical particles, uniformly distributed in the nano-range. The spherical shape of CS-PAA particles was also reported in the work of Wu et al., (Wu et al., 2017b).

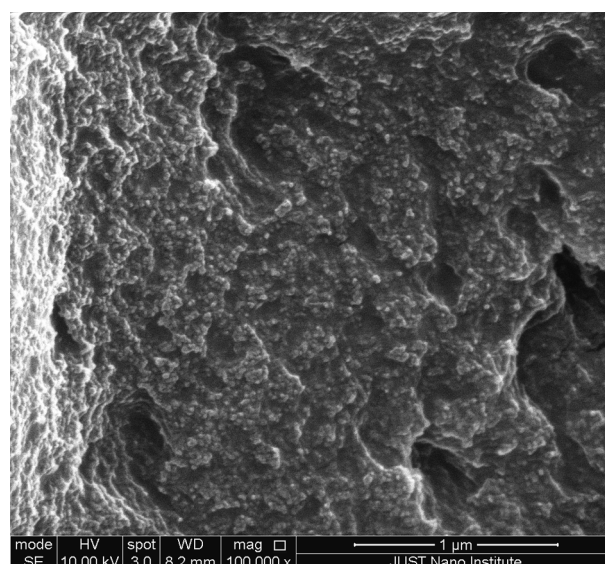


Fig. 1. SEM images of CS-PAA nanoparticles at 100,000 \times magnification.

3.3. Fourier transform infra-red (FT-IR) analysis

Fig. 2 shows the FTIR spectra of (a) CS, (b) PAA, and (c) CS-PAA nanoparticles. CS showed characteristic peaks at 3261 cm^{-1} related to O–H and at 1682 cm^{-1} related to C = O (amide). The peaks at 2928 and 1200 cm^{-1} were assigned for C–H and C–O bond stretching in PAA, respectively (Kohestanian et al., 2022). For CS-PAA nanoparticles, a new absorption peak emerged at 1628 cm^{-1} related to the $-\text{NH}_3^+$ absorption of CS. A broad peak also appeared at 2500 cm^{-1} which also confirmed the presence of NH_3^+ in CS-PAA nanoparticles. Moreover, the absorption peaks at 1532 cm^{-1} and 1414 cm^{-1} could be related to asymmetric and symmetric stretching vibrations of COO^- groups. The superimposed peak at 3261 cm^{-1} represented stretching vibrations of $-\text{OH}$, $-\text{NH}$ and intermolecular hydrogen bonding.

3.4. *Campylobacter jejuni* biofilm formation in pure culture and in mixed culture with *P. aeruginosa* and *E. coli*

Using the crystal violet staining method, biofilms of *C. jejuni* ATCC 33560, *P. aeruginosa* ATCC 12453, and *E. coli* ATCC 25922 were detected in individual or mixed cultures on 96-well plates under aerobic conditions at $37\text{ }^\circ\text{C}$ for 48 h. Data revealed that when *C. jejuni* was co-cultivated with either *P. aeruginosa* or *E. coli* or both, considerably more biofilms were produced, which demonstrated that the mixed culture biofilms included more living cells than the pure culture biofilms (Fig. 3).

3.5. Effect of CS-PAA nanoparticles on biofilm formation

When *C. jejuni* ATCC 33560 was treated with the CS-PAA nanoparticles under aerobic conditions at $37\text{ }^\circ\text{C}$, biofilm formation was inhibited. As shown in Fig. 4, a significant inhibitory effect was detected at a concentration of CS-PAA nanoparticles of 0.5 mg/mL , with a *P* value of 0.0008 . The effect of CS-PAA nanoparticles on biofilm formation was also assessed by visualizing bacterial cells stained with crystal violet. Light microscopy indicated the disruption of biofilm architecture after treatment for 24 h, resulting in decreased biofilm formation at $40\text{ }\mu\text{g}$ CS-PAA, whereas the control well exhibited dense biofilm formation (Fig. 5).

3.6. Antimicrobial activity of CS-PAA nanoparticles

The agar-well diffusion assay manifested the significant antimicrobial activity of CS-PAA nanoparticles against the tested clinical isolates. Indeed, agar-well diffusion assay showed that $20\text{ }\mu\text{g}$ of CS-PAA nanoparticles effectively inhibited the growth of *C. jejuni* ATCC 33560, *P. aeruginosa* ATCC 12453, and *E. coli* ATCC 25922 (Fig. 6). Antibacterial

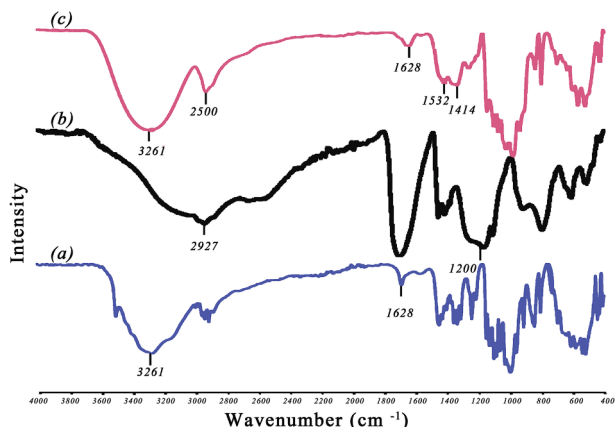


Fig. 2. FT-IR spectra of (a) CS, (b) PAA, and (c) CS-PAA nanoparticles.

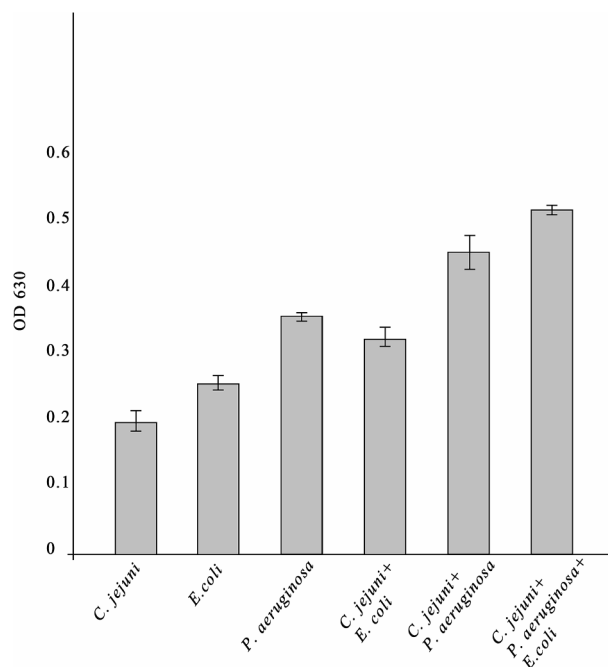


Fig. 3. Pure and mixed cultures of the aerobically tested bacteria *C. jejuni* ATCC 33560, *P. aeruginosa* ATCC 12453, and *E. coli* ATCC 25922 were compared for biofilm formation. In 96-well plates under aerobic conditions at $37\text{ }^\circ\text{C}$ for 48 h, biofilm development was evaluated using crystal violet staining and optical density (OD) measurements. The bars on the graph represent mean \pm SD of biofilm formation from three independent experiments. The ANOVA test showed a statically significant difference relative to the control ($p < 0.05$). (For interpretation of the references to colour in this figure legend, the reader is referred to the web version of this article.)

activity of CS-PAA nanoparticles was almost similar against all tested isolates ($P < 0.01$). However, maximum activity was noticed against *E. coli* with zone of inhibition (mm) of $13\text{ mm} \pm 0.62$ followed by *P. aeruginosa* ($12\text{ mm} \pm 0.4$), *C. jejuni* ($9.0\text{ mm} \pm 0.0$), Table 1.

4. Discussion

CS is the most important derivative of chitin, produced by removing the acetate moiety from chitin. The source of chitosan is the cell walls of fungi, as well as the shells of crustaceans like crabs and prawns (Mohammed et al., 2017). Here, CS-nanoparticles were synthesized through the ionic gelation of chitosan with tripolyphosphate anions. Particle sizing can be initially perplexing considering the diverse range of methods and corresponding devices. The size of CS-PAA nanoparticles is highly dependent on the preparation conditions, such as the pH of the preparation media and the concentrations of CS, TPP, and PAA (Liu and Gao, 2009). In this context, the herein findings indicate that the freeze-drying process imposed stress on the particles during preparation, leading to an observed increase in particles size (Costa et al., 2023). The significant difference between the two measurements could be related to the fact that SEM measurements capture conformations in the dry state, whereas those obtained through laser diffraction reflect the hydrodynamic diameter. Moreover, chitosan regions uncoated by the PAA experience swelling, which could falsify the particle size measurement (Spindler et al., 2021). The ZP values of the particles were $+45.85$ and $+16.39\text{ mV}$ for CS-TPP and CS-PAA, respectively. The difference in values may be attributed to the reduction of the number of free amino groups on CS due to the grafting of PAA. This signifies the formation of the CS-PAA nanoparticles (Hu et al., 2007). However, some chitosan chains were in excess and contributed to the stability of the particles (Zheng et al., 2007). ART-FTIR confirmed the formation of the CS-PAA complex. The presence of $-\text{NH}_3^+$ in CS-PAA was substantiated by the

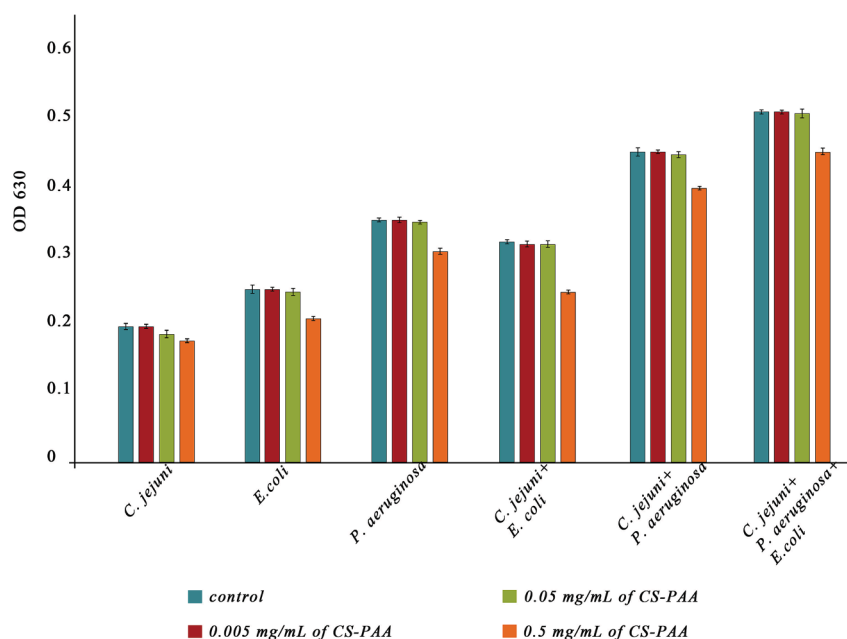


Fig. 4. Pure and mixed cultures were evaluated for biofilm suppression by different concentration of CS-PAA nanoparticles measured under aerobic conditions. The bars on the graph represent mean \pm SD of biofilm formation from three independent experiments. The ANOVA test showed a statically significant difference relative to the control ($p < 0.01$).

existence of peaks at 1628 cm^{-1} , which is originally related to the $-\text{NH}_3^+$ absorption of CS, and at 2500 cm^{-1} . Conversely, peaks at 1532 cm^{-1} and 1414 cm^{-1} indicated the presence of COO^- groups. The superimposed peak at 3261 cm^{-1} demonstrated the presence of intermolecular hydrogen bonding (Xu et al., 2014). These results suggest that the COOH groups of PAA dissociated into COO^- groups, which then complexed with the $-\text{NH}_3^+$ of CS through electrostatic interaction to form the CS-PAA nanoparticles.

The results of *C. jejuni* biofilm formation in pure culture and in mixed culture with *P. aeruginosa* and *E. coli* are comparable with a previous report where *C. jejuni* was co-cultured with *E. coli* and *P. aeruginosa* and the survival rate of *C. jejuni* found to be increased due to the presence of other strains (Zhong et al., 2020). In this context, co-culturing with several types of microorganisms, as often occurs in natural settings, could enhance the environmental conditions by reducing the concentrations of oxygen and altering the secondary metabolite levels (Wu et al., 2016). Definitely, microbial co-culture, which includes growing two or more microorganisms in the same small space, has been addressed as a potential method for triggering cryptic pathways (Selegato and Castro-Gamboa, 2023). A previous studies proved different types of microorganisms, such as *Saccharomyces cerevisiae*, a species of yeast, and *Lactobacillus plantarum*, a strain of probiotics, could form a mixed-species biofilm on a glass surface in liquid media to improve their capacity and endure challenging conditions (Furukawa et al., 2015; NOZAKA et al., 2014; Yin et al., 2019). A Recent study has demonstrated that, in co-culture, diffusible signal factor (DSF) or auto regulatory molecules can influence biofilm architecture, stress response, and polymyxins tolerance in *P. aeruginosa*. Similar outcomes have been observed with the DSF α,β -unsaturated fatty acid *cis*-2-dodecenoic acid (BDSF) generated by *Burkholderia cenocepacia*, which inhibited *C. albicans* germ tube growth while restoring biofilm and extracellular polysaccharide synthesis in *X. campestris* (Selegato and Castro-Gamboa, 2023).

The phenomenon of bacterial biofilm resistance to antimicrobials is an essential topic for several research projects that focus on alternative sources of biocompatible materials from living organisms. Previously, it has been shown that chemically altered chitosan derivatives involving N- and O-substitution, copolymerization, and grafting were effective

against biofilm forming bacteria. However, the underlying processes are not fully understood (Khan et al., 2020). According to Sahariah et al., the addition of lipophilic moieties to quaternary ammonium-modified chitosan, significantly improves the antibiofilm effectiveness of the material. The most effective antibiofilm against *S. aureus* was N-Acetyl-N-stearoyl-N',N'',N-trimethyl chitosan, which has two hydrophobic groups, acetyl and stearoyl (Sahariah et al., 2018). Because of its enhanced ability to penetrate biofilms, N-acetyl-N-stearoyl-N', N'',N''-trimethyl chitosan exhibits a reduction of up to four-fold in minimum biofilm eradication concentration (MBEC) compared to a control lacking lipophilic components (Si et al., 2022).

Previously, it was shown that ZnO nanoparticles had an antibiofilm effect. This is due to the fact that ZnO nanoparticles are small and have a large specific surface area, and have a high oxidation ability (Alves et al., 2017). The results of this study were comparable with Thaya et al. (2018), whose antibiofilm activity results demonstrated that chitosan-alginate (CS/ALG) microspheres inhibited the bacterial biofilm formation in *S. aureus*, *E. faecalis*, *P. aeruginosa* and *P. vulgaris* after a single treatment with $40\text{ }\mu\text{g}$. As chitosan possesses a positive charge, it can easily react with the cell membrane of negatively charged bacteria and compromise bacterial cell membrane permeability as well as interfere with membrane proteins, thereby affecting its structure and function (Thaya et al., 2018). According to the data from the light microscopy test, CS-PAA nanoparticles obstruct the biofilm layer and exhibit actual potential inhibition. Similarly, chitosan nanoparticles containing various chitosan types, such as low- and high-molecular mass chitosan substances, had an antibacterial action that prevented the growth of bacterial biofilms (Pintado, 2014).

The CS-PAA nanoparticles, prepared by employing chitosan, exhibited an efficient antibacterial activity against three-gram negative strains. The cationic nature of the CS-PAA nanoparticles enhanced the absorption into the negatively charged cell membranes of pathogenic bacteria (Ortega et al., 2010). Indeed, the complex might protect the chitosan from being degraded by glycoside hydrolyze enzymes such as chitinases or chitosanases that are produced by these bacteria (Yang et al., 2003). A recent study exhibited potent inhibition against *S. aureus* and *E. coli* using CS-nanoparticles in the presence of TPP (Al-Zahrani et al., 2021). Notably, compared to commercial antibiotics, chitosan

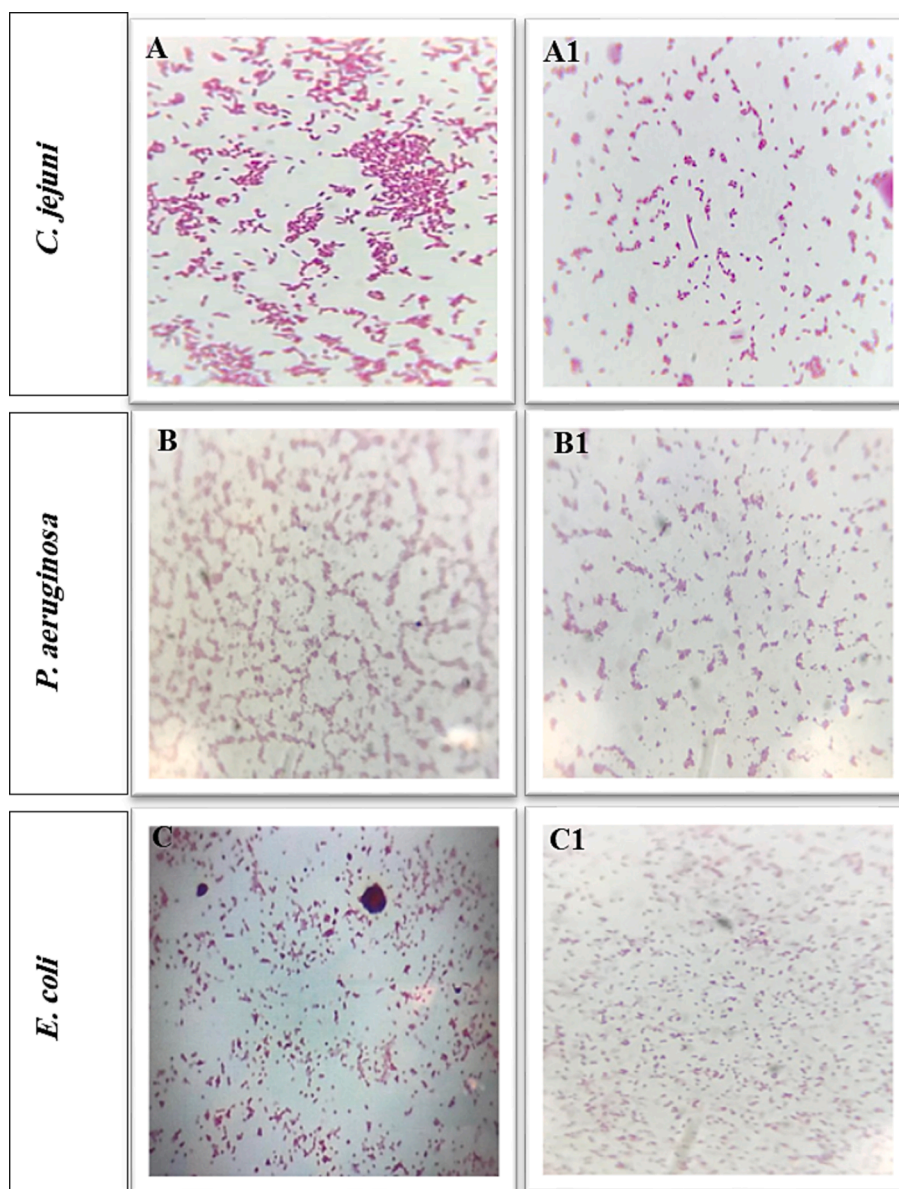


Fig. 5. Microscopic visualization (40X) of biofilm formation against clinical pathogens, *C. jejuni* ATCC 33560 (A), *P. aeruginosa* ATCC 12453 (B), and *E. coli* ATCC 25922 (C), without CS-PAA microspheres (A, B, and C) vs treated with 40 µg of CS-PAA microspheres concentration, showing the inhibition of biofilm formation (A1, B1 and C1).

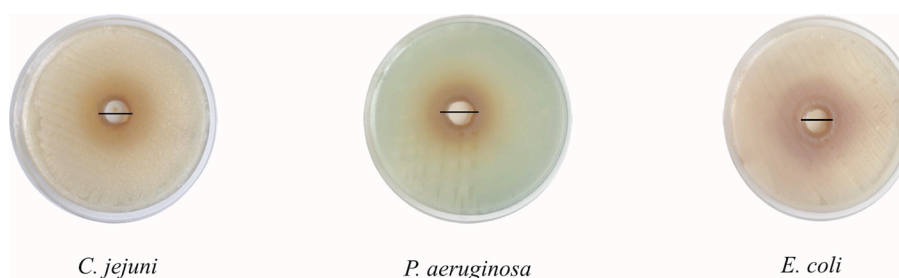


Fig. 6. Agar well diffusion assay for the determination of antibacterial activity of CS-PAA nanoparticles. White arrows indicate the zone of inhibition (mm) produced by CS-PAA nanoparticles against clinical pathogens, *C. jejuni* ATCC 33560, *P. aeruginosa* ATCC 12453, and *E. coli* ATCC 25922.

compounds exhibiting a high degree of substitution and medium molecular weight exhibited superior antibacterial activity. Furthermore, it was demonstrated that chitosan with varying molecular weights exhibited enhanced antibacterial activity when the degree of

substitution was increased (Kritchenkov et al., 2020). However, it has been demonstrated that other polymers, such as starch and starch-stabilized Ag nanoparticles, exhibit effective antibacterial activity, being less or non-toxic to mammalian macrophages at bactericidal

Table 1
Antibacterial activity CS-PAA nanoparticles against tested clinical isolates.

Name of the Strains	Zone of Inhibition (mm)
<i>C. jejuni</i> ATCC 33560	9.0 mm ± 0.0
<i>P. aeruginosa</i> ATCC 12453	12 mm ± 0.4
<i>E. coli</i> ATCC 25922	13 mm ± 0.62

concentrations that disrupt biofilm formation and eradicate intracellular mycobacteria. This was associated with the human cationic antimicrobial peptide LL-37 (Mohanty et al., 2012). The inhibitory impact on bacterial growth results from the ability of positively charged chitosan to disrupt the negatively charged cell membranes of bacteria (Kumbar et al., 2002; Wang et al., 2012). It is worth to mention that, understanding the antibacterial mechanism becomes challenging due to variations in cell surface characteristics between Gram-positive and Gram-negative bacteria (Yilmaz Atay, 2020).

5. Conclusion

Nanoparticles have been emerged as innovative tools providing an effective alternative to antibiotics for combating deadly bacterial infections directly or indirectly. CS has also been explored as a drug carrier due to its biocompatible properties. In this study, cationic CS-PAA nanoparticles were prepared by crosslinking PAA on the surface of CS-TPP particles. The resulting nanoparticles were spherical in shape and had a particle size of approximately 222 nm. This nano-system showed superior antibiofilm activity and antimicrobial effects against different gram-negative bacterial strains. These promising results position this novel system as low-cost, safe, and effective potential strategy against bacterial infections and a possible carrier for antibacterial drugs for augmented activity. However, since using nanoparticles is still relatively new, careful consideration of risks is essential. *In vitro* tests should address key properties of the CS-PAA, their biopersistence and possible mechanisms in the future.

Declaration of Competing Interest

The authors declare that they have no known competing financial interests or personal relationships that could have appeared to influence the work reported in this paper.

Acknowledgement

The research reported in this publication was funded by the Deanship of Scientific Research and Innovation at Al-Balqa Applied University in Jordan under Award Number 659/2020/ 2021.

References

- Abd El-Aziz, M.E., Morsi, S.M.M., Kamal, K.H., Khattab, T.A., 2022. Preparation of Isopropyl Acrylamide Grafted Chitosan and Carbon Bionanocomposites for Adsorption of Lead Ion and Methylene Blue. *Polymers (Basel)*. 14, 4485.
- Abd El-Aziz, M.E., Youssef, A.M., Kamal, K.H., Kelnar, I., Kamel, S., 2023. Preparation and performance of bionanocomposites based on grafted chitosan, GO and TiO₂-NPs for removal of lead ions and basic-red 46. *Carbohydr. Polym.* 305, 120571.
- Ahmed, N.J., Haseeb, A., AlQarni, A., Algethamy, M., Mahrous, A.J., Alshehri, A.M., Alahmari, A.K., Abuhussain, S.S., Mohammed Bashawri, A., Khan, A.H., 2023. Antibiotics for Preventing Infection at the Surgical Site: Single Dose vs. Multiple Doses. *Saudi Pharm. J.* 101800 <https://doi.org/10.1016/j.jps.2023.101800>.
- Alalawi, A., Carpinone, P., Alshahrani, S., Alsulays, B., Ansari, M., Anwer, M., Alshehri, S., Alshetaili, A., 2019. Influence of chitosan coating on the oral bioavailability of gold nanoparticles in rats. *Saudi Pharm. J.* 27, 171–175. <https://doi.org/10.1016/j.jps.2018.09.011>.
- Al-khreshieh, R.O., Al-fawares, O., Em, A., 2023. Campylobacter jejuni Infections : Epidemiology, Pathophysiology, Clinical Manifestations and Management. *J. Biomed. Res. Environ. Sci.* 4 <https://doi.org/10.37871/jbres1670>.
- Alves, M.M., Bouchami, O., Tavares, A., Córdoba, L., Santos, C.F., Miragaia, M., de Fátima Montemor, M., 2017. New Insights into Antibiofilm Effect of a Nanosized ZnO Coating against the Pathogenic Methicillin Resistant Staphylococcus aureus.

- ACS Appl. Mater. Interfaces 9, 28157–28167. <https://doi.org/10.1021/acsami.7b02320>.
- Al-Zahrani, S.S., Bora, R.S., Al-Garni, S.M., 2021. Antimicrobial activity of chitosan nanoparticles. *Biotechnol. Biotechnol. Equip.* 35, 1874–1880.
- Anjugam, M., Iswarya, A., Vaseeharan, B., 2016. Multifunctional role of β-1, 3 glucan binding protein purified from the haemocytes of blue swimmer crab Portunus pelagicus and in vitro antibacterial activity of its reaction product. *Fish Shellfish Immunol.* 48, 196–205. <https://doi.org/10.1016/j.fsi.2015.11.023>.
- Belbekhouche, S., Mansour, O., Carbonnier, B., 2018. Promising sub-100 nm tailor made hollow chitosan/poly (acrylic acid) nanocapsules for antibiotic therapy. *J. Colloid Interface Sci.* 522, 183–190.
- Cheung, R.C.F., Ng, T.B., Wong, J.H., Chan, W.Y., 2015. Chitosan: an update on potential biomedical and pharmaceutical applications. *Mar. Drugs* 13, 5156–5186.
- Costa, E.M., Silva, S., Pintado, M., 2023. Chitosan Nanoparticles Production: Optimization of Physical Parameters, Biochemical Characterization, and Stability upon Storage. *Appl. Sci.* 13 <https://doi.org/10.3390/app13031900>.
- Elgamoudi, B.A., Korolik, V., 2021. Campylobacter Biofilms: Potential of Natural Compounds to Disrupt Campylobacter jejuni Transmission. *Int. J. Mol. Sci.* 22 <https://doi.org/10.3390/ijms222212159>.
- Esim, O., Savaser, A., Ozkan, C.K., Bayrak, Z., Tas, C., Ozkan, Y., 2018. Effect of polymer type on characteristics of buccal tablets using factorial design. *Saudi Pharm. J.* 26, 53–63. <https://doi.org/10.1016/j.jps.2017.10.013>.
- Fredin, N.J., Zhang, J., Lynn, D.M., 2005. Surface analysis of erodible multilayered polyelectrolyte films: Nanometer-scale structure and erosion profiles. *Langmuir* 21, 5803–5811.
- Furukawa, S., Isomae, R., Tsuchiya, N., Hirayama, S., Yamagishi, A., Kobayashi, M., Suzuki, C., Ogihara, H., Morinaga, Y., 2015. Screening of lactic acid bacteria that can form mixed-species biofilm with Saccharomyces cerevisiae. *Biosci. Biotechnol. Biochem.* 79, 681–686. <https://doi.org/10.1080/09168451.2014.991691>.
- Hu, Y., Ding, Y., Ding, D., Sun, M., Zhang, L., Jiang, X., Yang, C., 2007. Hollow chitosan/poly (acrylic acid) nanospheres as drug carriers. *Biomacromolecules* 8, 1069–1076.
- Hughes, G., Webber, M.A., 2017. Novel approaches to the treatment of bacterial biofilm infections. *Br. J. Pharmacol.* 174, 2237–2246. <https://doi.org/10.1111/bph.13706>.
- Ijaz, H., Tulain, U.R., Minhas, M.U., Mahmood, A., Sarfraz, R.M., Erum, A., Danish, Z., 2022. Design and in vitro evaluation of pH-sensitive crosslinked chitosan-grafted acrylic acid copolymer (CS-co-AA) for targeted drug delivery. *Int. J. Polym. Mater. Polym. Biomater.* 71, 336–348.
- Kamat, S., Kumari, M., 2023. Emergence of microbial resistance against nanoparticles: Mechanisms and strategies. *Front. Microbiol.* 14 <https://doi.org/10.3389/fmicb.2023.1102615>.
- Karolewicz, B., 2016. A review of polymers as multifunctional excipients in drug dosage form technology. *Saudi Pharm. J.* 24, 525–536. <https://doi.org/10.1016/j.jps.2015.02.025>.
- Karruli, A., Catalini, C., D'Amore, C., Foglia, F., Mari, F., Harxhi, A., Galdiero, M., Durante-Mangoni, E., 2023. Evidence-Based Treatment of Pseudomonas aeruginosa Infections: A Critical Reappraisal. *Antibiotics* 12. <https://doi.org/10.3390/antibiotics12020399>.
- Kemper, L., Hensel, A., 2023. Campylobacter jejuni: targeting host cells, adhesion, invasion, and survival. *Appl. Microbiol. Biotechnol.* 2725–2754 <https://doi.org/10.1007/s00253-023-12456-w>.
- Khan, F., Pham, D.T.N., Oloketuyi, S.F., Manivasagan, P., Oh, J., Kim, Y.-M., 2020. Chitosan and their derivatives: Antibiofilm drugs against pathogenic bacteria. *Colloids Surfaces B Biointerfaces* 185, 110627. <https://doi.org/10.1016/j.colsurfb.2019.110627>.
- Kim, J., Park, H., Kim, J., Kim, J.H., Jung, J.I., Cho, S., Ryu, S., Jeon, B., 2019. Comparative Analysis of Aerotolerance, Antibiotic Resistance, and Virulence Gene Prevalence in Campylobacter jejuni Isolates from Retail Raw Chicken and Duck Meat in South Korea. *Microorganisms* 7. <https://doi.org/10.3390/microorganisms7100433>.
- Kohestanian, M., Boughendi, H., Keshavarzi, N., Mahmoudi, M., Pourjavadi, A., Ghiassi, M., 2022. Preparation of poly (acrylic acid) microgels by alcohol type cross-linkers and a comparison with other cross-linking methods. *Polym. Bull.* 1–20.
- Kritchenkov, A.S., Egorov, A.R., Artemjev, A.A., Kritchenkov, I.S., Volkova, O.V., Kurliuk, A.V., Shakola, T.V., Rubanik Jr, V.V., Rubanik, V.V., Tskhovrebov, A.G., 2020. Ultrasound-assisted catalyst-free thiol-yne click reaction in chitosan chemistry: Antibacterial and transfection activity of novel cationic chitosan derivatives and their based nanoparticles. *Int. J. Biol. Macromol.* 143, 143–152.
- Kumbar, S.G., Kulkarni, A.R., Aminabhavi, M., 2002. Crosslinked chitosan microspheres for encapsulation of diclofenac sodium: effect of crosslinking agent. *J. Microencapsul.* 19, 173–180. <https://doi.org/10.1080/02652040110065422>.
- Liu, H., Gao, C., 2009. Preparation and properties of ionically cross-linked chitosan nanoparticles. *Polym. Adv. Technol.* 20, 613–619. <https://doi.org/10.1002/pat.1306>.
- Mancuso, G., Midiri, A., Gerace, E., Biondo, C., 2021. Bacterial Antibiotic Resistance: The Most Critical Pathogens. *Pathog. (Basel, Switzerland)* 10. <https://doi.org/10.3390/pathogens10101310>.
- Mohammed, M.A., Syeda, J.T.M., Wasan, K.M., Wasan, E.K., 2017. An overview of chitosan nanoparticles and its application in non-parenteral drug delivery. *Pharmaceutics* 2017 (9), 53.
- Mohanty, S., Mishra, S., Jena, P., Jacob, B., Sarkar, B., Sonawane, A., 2012. An investigation on the antibacterial, cytotoxic, and antibiofilm efficacy of starch-stabilized silver nanoparticles. *Nanomedicine* 8, 916–924. <https://doi.org/10.1016/j.nano.2011.11.007>.
- Mu, H., Guo, F., Niu, H., Liu, Q., Wang, S., Duan, J., 2014a. Chitosan improves anti-biofilm efficacy of gentamicin through facilitating antibiotic penetration. *Int. J. Mol. Sci.* 15, 22296–22308.

- Mu, H., Zhang, A., Zhang, L., Niu, H., Duan, J., 2014b. Inhibitory effects of chitosan in combination with antibiotics on *Listeria monocytogenes* biofilm. *Food Control* 38, 215–220.
- MubarakAli, D., Arunkumar, J., Pooja, P., Subramanian, G., Thajuddin, N., Alharbi, N.S., 2015. Synthesis and characterization of biocompatibility of tenorite nanoparticles and potential property against biofilm formation. *Saudi Pharm. J.* 23, 421–428. <https://doi.org/10.1016/j.jsps.2014.11.007>.
- Nozaka, S., Furukawa, S., Sasaki, M., Hirayama, S., Ogihara, H., Morinaga, Y., 2014. Manganese Ion Increases LAB-yeast Mixed-species Biofilm Formation. *Biosci. Microbiota, Food Heal.* 33, 79–84. <https://doi.org/10.12938/bmfh.33.79>.
- Oh, E., Andrews, K.J., McMullen, L.M., Jeon, B., 2019. Tolerance to stress conditions associated with food safety in *Campylobacter jejuni* strains isolated from retail raw chicken. *Sci. Rep.* 9, 11915. <https://doi.org/10.1038/s41598-019-48373-0>.
- Ortega, H., Gutiérrez, B., Cadenas, G., Ibarra, L., 2010. Antibacterial Activity of Interpolyelectrolyte Complexes Chitosan Chitosan and the of Poly (acrylic acid) -. *Braz Arch Biol Techn* 53, 623–628.
- Ortega-Ortiz, H., Gutiérrez-Rodríguez, B., Cadenas-Pliego, G., Jimenez, L.I., 2010. Antibacterial activity of chitosan and the interpolyelectrolyte complexes of poly (acrylic acid)-chitosan. *Brazilian Arch. Biol. Technol.* 53, 623–628.
- Paulsamy, P., Venkatesan, K., Hamoud Alshahrani, S., Hamed Mohamed Ali, M., Prabakar, K., Prabhu Veeramani, V., Khalil Elfaki, N., Elsayed Ahmed, R., Ahmed Elsayes, H., Hussein Ahmed Abdalla, Y., Babiker Osmsn Mohammed, O., Ahmed Qureshi, A., Alqahtani, F., Shaik Alavudeen, S., 2023. Parental health-seeking behavior on self-medication, antibiotic use, and antimicrobial resistance in children. *Saudi Pharm. J.* 31, 101712. <https://doi.org/https://doi.org/10.1016/j.jsps.2023.101712>.
- Pintado, M., 2014. Antimicrobial Effect of Chitosan against Periodontal Pathogens Biofilms. *SOJ Microbiol. Infect. Dis.* 2 <https://doi.org/10.15226/sojmid.2013.00114>.
- Radwan, A.A., Al-Anazi, F.K., Al-Agamy, M., Alghaith, A.F., Mahrous, G.M., Alhuzani, M. R., Alghamdi, A.S.A., 2023. Design, synthesis and molecular modeling of isatin-aminobenzoic acid hybrids as antibacterial and antibiofilm agents. *Saudi Pharm. J.* 101781 <https://doi.org/10.1016/j.jsps.2023.101781>.
- Sahariah, P., Måsson, M., Meyer, R.L., 2018. Quaternary Ammoniumyl Chitosan Derivatives for Eradication of *Staphylococcus aureus* Biofilms. *Biomacromolecules* 19, 3649–3658. <https://doi.org/10.1021/acs.biomac.8b00718>.
- Selegato, D.M., Castro-Gamboa, I., 2023. Enhancing chemical and biological diversity by co-cultivation. *Front. Microbiol.* 14, 1–24. <https://doi.org/10.3389/fmicb.2023.1117559>.
- Si, Z., Zheng, W., Prananty, D., Li, J., Koh, C.H., Kang, E.-T., Pethe, K., Chan-Park, M.B., 2022. Polymers as advanced antibacterial and antibiofilm agents for direct and combination therapies. *Chem. Sci.* 13, 345–364. <https://doi.org/10.1039/d1sc05835e>.
- Siddhardha, B., Pandey, U., Kaviyarasu, K., Pala, R., Syed, A., Bahkali, A.H., Elgorban, A. M., 2020. Chrysin-loaded chitosan nanoparticles potentiates antibiofilm activity against *Staphylococcus aureus*. *Pathogens* 9, 115.
- Spindler, L.M., Feuerhake, A., Ladel, S., Günday, C., Flamm, J., Günday-Türeli, N., Türeli, E., Tovar, G.E.M., Schindowski, K., Gruber-Traub, C., 2021. Nano-in-Micro-Particles Consisting of PLGA Nanoparticles Embedded in Chitosan Microparticles via Spray-Drying Enhances Their Uptake in the Olfactory Mucosa. *Front. Pharmacol.* 12, 1–19. <https://doi.org/10.3389/fphar.2021.732954>.
- Stetsenko, V.V., Efimochkina, N.R., Pichugina, T.V., 2019. Growth and Persistence of *Campylobacter jejuni* in Foodstuffs. *Bull. Exp. Biol. Med.* 166, 759–765. <https://doi.org/10.1007/s10517-019-04435-x>.
- Sultan, M.H., Moni, S.S., Alqahtani, S.S., Ali Bakkari, M., Alshammari, A., Almohari, Y., Alshahrani, S., Madkhali, O.A., Mohan, S., 2023. Design, physicochemical characterisation, and in vitro cytotoxicity of cisplatin-loaded PEGylated chitosan injectable nano / sub-micron crystals. *Saudi Pharm. J.* 31, 861–873. <https://doi.org/10.1016/j.jsps.2023.04.005>.
- Suwono, B., Hammerl, J.A., Eckmanns, T., Merle, R., Eigner, U., Lümen, M., Lauter, S., Stock, R., Fenner, I., Boemke, E., Tenhagen, B.-A., 2021. Comparison of MICs in *Escherichia coli* isolates from human health surveillance with MICs obtained for the same isolates by broth microdilution. *JAC-antimicrobial Resist.* 3, dlab145. <https://doi.org/10.1093/jacamr/dlab145>.
- Thaya, R., Vaseeharan, B., Sivakamavalli, J., Iswarya, A., Govindarajan, M., Alharbi, N. S., Kadaikunnan, S., Al-anbr, M.N., Khaled, J.M., Benelli, G., 2018. Synthesis of chitosan-alginate microspheres with high antimicrobial and antibiofilm activity against multi-drug resistant microbial pathogens. *Microb. Pathog.* 114, 17–24. <https://doi.org/10.1016/j.micpath.2017.11.011>.
- TopuzoGullari, M., 2020. Effect of polyelectrolyte complex formation on the antibacterial activity of copolymer of alkylated 4-vinylpyridine. *Turkish J. Chem.* 44, 634–646.
- Wang, Y., Li, L., Li, B., Wu, G., Tang, Q., Ibrahim, M., Li, H., Xie, G., Sun, G., 2012. Action of Chitosan Against *Xanthomonas* Pathogenic Bacteria Isolated from *Euphorbia pulcherrima*. *Molecules* 17, 7028–7041. <https://doi.org/10.3390/molecules17067028>.
- Wu, Y., Wu, J., Cao, J., Zhang, Y., Xu, Z., Qin, X., Wang, W., Yuan, Z., 2017a. Facile fabrication of poly (acrylic acid) coated chitosan nanoparticles with improved stability in biological environments. *Eur. J. Pharm. Biopharm.* 112, 148–154.
- Wu, Y., Wu, J., Cao, J., Zhang, Y., Xu, Z., Qin, X., Wang, W., Yuan, Z., 2017b. Facile fabrication of poly(acrylic acid) coated chitosan nanoparticles with improved stability in biological environments. *Eur. J. Pharm. Biopharm.* 112, 148–154. <https://doi.org/10.1016/j.ejpb.2016.11.020>.
- Wu, Q., Zhong, X., Zhang, J., 2016. Research progress in biofilm formation and regulatory mechanism of *Campylobacter jejuni*. *Wei Sheng Wu Xue Bao* 56, 180–187.
- Xiao, L., Wang, B., Yang, G., Gauthier, M., 2012. Poly (lactic acid)-based biomaterials: synthesis, modification and applications. *Biomed. Sci. Eng. Technol.* 11, 247–282.
- Xu, J., Lin, Q., Sheng, M., Ding, T., Li, B., Gao, Y., Tan, Y., 2022. Antibiofilm Effect of Cinnamaldehyde-Chitosan Nanoparticles against the Biofilm of *Staphylococcus aureus*. *Antibiot. (Basel, Switzerland)* 11. <https://doi.org/10.3390/antibiotics11101403>.
- Xu, X.-M., Xu, J.-H., Wu, H.-C., Luo, G.-S., 2014. Microfluidic preparation of chitosan-poly(acrylic acid) composite microspheres with a porous surface structure. *RSC Adv.* 4, 37142–37147. <https://doi.org/10.1039/C4RA06328G>.
- Yang, J.-M., Lin, H.T., Wu, T.H., Chen, C., 2003. Wettability and antibacterial assessment of chitosan containing radiation-induced graft nonwoven fabric of polypropylene-g-acrylic acid. *J. Appl. Polym. Sci.* 90, 1331–1336.
- H. Yilmaz Atay Antibacterial Activity of Chitosan-Based Systems 2020 Chitosan Drug Deliv. *Biomed. Appl Funct* 10.1007/978-981-15-0263-7_15.
- Yin, W., Wang, Y., Liu, L., He, J., 2019. Biofilms: The Microbial “Protective Clothing” in Extreme Environments. *Int. J. Mol. Sci.* 20 <https://doi.org/10.3390/ijms20143423>.
- Zheng, Y., Yang, W., Wang, C., Hu, J., Fu, S., Dong, L., Wu, L., Shen, X., 2007. Nanoparticles based on the complex of chitosan and polyaspartic acid sodium salt: preparation, characterization and the use for 5-fluorouracil delivery. *Eur. J. Pharm. Biopharm. Off. J. Arbeitsgemeinschaft fur Pharm. Verfahrenstechnik e.V* 67, 621–631. <https://doi.org/10.1016/j.ejpb.2007.04.007>.
- Zhong, X., Wu, Q., Zhang, J., Ma, Z., Wang, J., Nie, X., Ding, Y., Xue, L., Chen, M., Wu, S., Wei, X., Zhang, Y., 2020. *Campylobacter jejuni* Biofilm Formation Under Aerobic Conditions and Inhibition by ZnO Nanoparticles. *Front. Microbiol.* 11, 1–6. <https://doi.org/10.3389/fmicb.2020.00207>.